System Reliability Analysis of Slope Stability Using Generalized Subset Simulation

Dian-Qing Li, Zhi-Yong Yang, Zi-Jun Cao*

State Key Laboratory of Water Resources and Hydropower Engineering Science, Key Laboratory of Rock Mechanics in Hydraulic Structural Engineering (Ministry of Education), Wuhan University, 8 Donghu South Road, Wuhan 430072, P. R. China.

Siu-Kui Au

Institute for Risk and Uncertainty, University of Liverpool, Harrison Hughes Building, Brownlow Hill, Liverpool, L69 3GH, United Kingdom

Kok-Kwang Phoon

Department of Civil and Environmental Engineering, National University of Singapore, Blk E1A, #07-03, 1 Engineering Drive 2, Singapore 117576, Singapore.

*Corresponding author

State Key Laboratory of Water Resources and Hydropower Engineering Science, Wuhan University, 8 Donghu South Road, Wuhan 430072, P. R. China.

Tel: (86)-27-6877 4036

Fax: (86)-27-6877 4295

E-mail: zijuncao@whu.edu.cn

Abstract

Slope failure mechanisms (e.g., why and where slope failure occurs) are usually unknown prior to slope stability analysis. Several possible failure scenarios (e.g., slope sliding along different slip surfaces) can be assumed, leading to a number of scenario failure events of slope stability. How to account rationally for various scenario failure events in slope stability reliability analysis and how to identify key failure events that have significant contributions to slope failure are critical questions in slope engineering. In this study, these questions are resolved by developing an efficient computer-based simulation method for slope system reliability analysis. The proposed approach decomposes a slope system failure event into a series of scenario failure events representing possible failure scenarios and calculates their occurrence probabilities by a single run of an advanced Monte Carlo simulation (MCS) method, called generalized Subset Simulation (GSS). Using GSS results, representative failure events (RFEs) that are considered relatively independent are identified from scenario failure events using probabilistic network evaluation technique. Their relative contributions are assessed quantitatively, based on which key failure events are determined. The proposed approach is illustrated using a soil slope example and a rock slope example. It is shown that the proposed approach provides proper estimates of occurrence probabilities of slope system failure event and scenario failure events by a single GSS run, which avoids repeatedly performing simulations for each failure event. Compared with direct MCS, the proposed approach significantly improves computational efficiency, particularly for failure events with small failure probabilities. Key failure events of slope stability are determined among scenario failure events in a cost-effective manner. Such information is valuable in making slope design decisions and remedial measures.

Keywords: Slope stability; Generalized Subset Simulation; System reliability; Representative failure event; Key failure event

1. Introduction

Various uncertainties exist in slope stability analysis, such as those in soil and rock properties, calculation models, loads, etc. (e.g., Christian et al., 1994; Baecher and Christian, 2003; Singh et al., 2013a; Wang et al., 2016; Cao et al., 2016; Li et al., 2016a). These uncertainties can be rationally taken into account in a probabilistic framework, where the plausibility of slope failure is quantified as the occurrence probability of soil or rock masses sliding along a slip surface, such as landslides and rock wedge sliding. Slope failure mechanisms are usually unknown prior to slope stability analysis with some exceptions, such as the cases with well-defined failure surfaces (e.g., Oka and Wu, 1990; Singh et al., 2012; Tang et al., 2015) or those concerned during post-failure investigations (e.g., El-Ramly et al., 2005). Several possible failure scenarios (e.g., slope sliding along different slip surfaces) can be assumed in slope stability analysis, leading to a number, n, of scenario failure events. These failure scenarios need to be properly incorporated into analysis to generate reasonable estimates of slope failure probability. Different failure scenarios may have different contributions to slope failure (e.g., Li et al., 2014; Kainthola et al., 2015). Identification of key failure events with significant contributions to slope failure is pivotal to making rational slope design decisions and remedial measures.

To account rationally for different slope failure scenarios, probabilistic slope stability analysis is commonly formulated as a system reliability problem (e.g., Ang and Tang, 1984). In the past two decades, several probabilistic analysis methods have been developed to evaluate system failure probability, $P(F)$, of soil and rock slopes, such as bound methods based on first order reliability method (FORM) (e.g., Oka and Wu, 1990; Chowdhury and Xu, 1995; Low, 1997; Jimenez-Rodriguez et al., 2006; Jimenez-Rodriguez and Sitar, 2007; Low et al., 2011; Zhang et al., 2011); modified FORMs considering multiple scenario failure events (e.g., Li et al., 2009, 2011a; Ji and Low, 2012; Cho, 2013; Zeng and Jimenez, 2014);

3

and direct Monte Carlo simulation (MCS) methods and its variants (e.g., Ching et al., 2009; Wang et al., 2011; Zhang et al., 2012, 2013; Li et al., 2013, 2014; Jiang et al., 2015; Li et al., 2016b,c). The accuracy of FORM-based bound methods and modified FORMs depends on the linearity of performance function governing slope failure and the number of scenario failure events (Ang and Tang, 1984; Low et al., 2011; Zeng and Jimenez, 2014). In contrast, direct MCS provides a conceptually simple tool for system reliability analysis of slope stability regardless of the linearity of performance function and the number of scenario failure events (e.g., Ching et al., 2009; Huang et al., 2010). More importantly, it is robust to various deterministic analysis methods for slope stability analysis, such as limit equilibrium methods, finite element methods, and finite difference methods (El-Ramly et al., 2005; Huang et al., 2010; Singh et al., 2013b). Nevertheless, direct MCS suffers from a lack of resolution and efficiency at small probability levels, which is of concern in slope design practice and necessitates extensive computational efforts to obtain reasonably accurate estimates of $P(F)$ (e.g., Baecher and Christian, 2003; Wang et al., 2010; Ji and Low, 2012).

The computational efficiency of MCS-based system reliability analysis of slope stability can be improved by two common strategies: (1) reducing the number of samples required in MCS by advanced sampling techniques, such as importance sampling (IS) (Ching et al., 2009) and Subset Simulation (Wang et al., 2011; Santoso et al., 2011; Li et al., 2016b,c); and (2) integrating MCS with surrogate models of deterministic slope stability analysis, such as response surfaces, artificial neural network etc. (Sinha et al., 2010; Li et al., 2011a,b; Zhang et al., 2011, 2012; Kang et al., 2015, 2016; Li et al., 2016d). These existing work only focused on efficient evaluation of $P(F)$, providing no insights into the relative contributions of different failure scenarios to slope system failure.

Li et al. (2013, 2014) proposed direct MCS-based approaches that decomposed $P(F)$ of soil slopes into those associated with a number of representative failure events (RFEs). These

methods can quantify the relative contributions of different RFEs to slope failure and identify the key failure events with significant contributions. Selecting RFEs of slope stability from scenario failure events requires knowledge of their failure probabilities (e.g., Zhang et al., 2011, 2012; Li et al., 2013, 2014). This necessitates repeatedly performing reliability analyses for different scenario failure events, which may not be a trivial task, particularly when the number of scenario failure events is large, e.g., for soil slopes. In addition, the accuracy of $P(F)$ estimated from RFEs depends on the number of selected RFEs whose determination is non-trivial before analysis.

This paper develops an efficient computer-based simulation method for slope system reliability analysis using an advanced MCS method called generalized Subset Simulation (GSS). The proposed method decomposes the system failure event F of slope stability into a number n of scenario failure events F_i, $i = 1, 2, \ldots, n$ through fault tree analysis (FTA), and calculates the system failure probability $P(F)$ and scenario failure probabilities $P(F_i)$ ($i = 1, 2, \ldots, n$) by a single run of GSS. This avoids repeatedly performing simulation for different failure events (e.g., F and F_i, $i = 1, 2, \ldots, n$), which can be time consuming when the number of slope failure events is large. The proposed method not only improves significantly the computational efficiency of calculating $P(F)$ and $P(F_i)$ at small probability levels, but also identifies the representative failure events and key failure events in a rational manner. As an additional advantage, the slope system failure probability is obtained from GSS prior to selecting RFEs, and so it is independent of RFEs, which allows determining the number of RFEs for representing slope system in a rational manner. This paper starts with development of the proposed approach. Then, the approach is illustrated using a soil slope example in Section 5 and a rock slope example in Section 6.

2. Fault Tree Analysis of System Failure of Slope Stability

Fault tree diagram is a graphical decomposition of system failure event into union and/or intersection of several scenario failure events that represent possible failure scenarios (e.g., Ang and Tang, 1984; Li et al., 2009). Figure 1 shows a fault tree diagram for system failure of slope stability, where the "*OR*" and "*AND*" gates indicate union and intersection of events, respectively. It consists of three levels: system level with a system failure event F of slope stability, failure scenario level with n scenario failure events (i.e., F_i, $i = 1, 2, \ldots, n$) representing possible failure scenarios, and component level that further decomposes each scenario failure event into a number j_i of components. As seen in Figure 1, slope system failure event F is formulated as the union of F_i, $i = 1, 2, \ldots, n$, i.e.,

$$F = F_1 \bigcup F_2 \bigcup \cdots \bigcup F_n = \{G_1 < 0\} \bigcup \{G_2 < 0\} \bigcup \cdots \bigcup \{G_n < 0\} \tag{1}$$

where G_i, $i = 1, 2, \ldots, n$, is the limit state function (LSF) of the i-th failure event $F_i = \{G_i < 0\}$. For slope stability analysis, G_i can be defined as $FS_i - 1$, where FS_i is the factor of safety of F_i. As indicated by Eq. (1), the occurrence of any scenario failure event F_i results in the slope failure. One can thus write $F = \{G_s < 0\}$, where $G_s = \min\{G_i, i = 1, 2, \ldots, n\}$. Without much loss of generality, F_i can be represented by the intersection of j_i component events:

$$F_i = \{g_{i,1} < 0\} \bigcap \{g_{i,2} < 0\} \bigcap \cdots \bigcap \{g_{i,j_i} < 0\}, \qquad i = 1, 2, \ldots, n \tag{2}$$

where $g_{i,l}$ = the LSF of the l-th component events. Based on Eq. (2), one can take $G_i = \max\{g_{i,l}, l = 1, 2, \ldots, j_i\}$.

The fault tree diagram in Figure 1 provides a flexible tool to describe soil and rock slope systems. For soil slopes, failure occurs if soil mass slides along any potential slip surfaces, each of which corresponds to a scenario failure event that usually has a single component, i.e., $j_i = 1$. The soil slope system is then described as a series system. For rock slopes, the scenario failure event may be further decomposed into several components, i.e., $j_i > 1$. Then, rock slope system can be represented by a combined series-parallel system.

Although n scenario failure events are identified through FTA, they may not be of equal importance to system failure. The key failure events with significant contributions to slope system failure shall be identified for making design decisions and remedial measures. This requires the knowledge of $P(F)$ and $P(F_i)$ ($i = 1, 2,…, n$), which are calculated by a single run of generalized Subset Simulation (GSS) (Li et al., 2015) in the next section.

3. Slope System Reliability Analysis Using Generalized Subset Simulation (GSS)

3.1. Original Subset Simulation algorithm

GSS is developed from the original Subset Simulation (SS) algorithm that focuses on efficiently evaluating the probability of a single rare failure event (Au and Beck, 2001, 2003a; Au and Wang, 2014). To facilitate understanding of GSS, this subsection describes the algorithm of the SS briefly. The SS algorithm expresses a rare failure event E with a small probability as a sequence of intermediate failure events $\{E^{(k)}, k = 1, 2, …, m\}$ with larger conditional failure probabilities (Au and Beck, 2001, 2003a; Li, 2011; Au and Wang, 2014). It employs specially designed Markov chains to generate conditional samples of these

intermediate failure events until the final target failure region is achieved. Let Y be the critical response of interest. Without loss of generality, define the rare event E as $E = \{Y < y\}$, where y is a given threshold value. Consider, for example, slope stability problem. The rare event E can be defined as the system failure (i.e., $E = F$) or the occurrence of a failure scenario (i.e., $E = F_i$). The corresponding critical responses are their respective values of LSFs, i.e., $Y = G_s$ for $E = F$ or $Y = G_i$ for $E = F_i$. Let $y^{(1)} > y^{(2)} > \ldots > y^{(m)} = y$ be a decreasing sequence of intermediate threshold values. The intermediate failure events $\{E^{(k)}, k = 1, 2, \ldots, m\}$ are then defined as $E^{(k)} = \{Y < y^{(k)}, k = 1, 2, \ldots, m\}$. By sequentially conditioning on these intermediate events, the occurrence probability $P(E)$ of E is written as (Au and Wang, 2014):

$$P(E) = P(E^{(m)}) = P(E^{(1)}) \prod_{k=2}^{m} P(E^{(k)} \mid E^{(k-1)}) \tag{3}$$

where $P(E^{(1)})$ is equal to $P(Y < y^{(1)})$, and $P(E^{(k)} \mid E^{(k-1)})$ is equal to $\{P(Y < y^{(k)} \mid Y < y^{(k-1)}), k = 2, 3, \ldots, m\}$. In implementations, $y^{(1)}, y^{(2)}, \ldots, y^{(m)}$ are generated adaptively using information from simulated samples so that the sample estimates of $P(E^{(1)})$ and $\{P(E^{(k)} \mid E^{(k-1)}), k = 2, 3, \ldots, m\}$ always correspond to a specified value of conditional probability p_0. The efficient generation of conditional samples is pivotal to the success of SS, and it is achieved using Markov Chain Monte Carlo simulation (MCMCS), as shown in Figure 2. Detailed implementation procedures of SS and descriptions on MCMCS are referred to (Au and Beck, 2001, 2003a; Au et al., 2010; Au and Wang, 2014; Li et al., 2016b,c).

Determining the intermediate failure events (i.e., $E^{(k)}, k = 1, 2, \ldots, m$) during SS depends on the pre-defined critical response Y, which is referred to as "driving variable"

8

(e.g., Wang and Cao, 2013; Li et al., 2016b,c). For a given Y, SS progressively drives sampling space to the domain with $E = \{Y < y\}$ and gives the corresponding $P(E)$. For example, using $Y = G_s$ and $Y = G_i$ in SS provides estimates of $P(F)$ for $E = F$ and $P(F_i)$ for $E = F_i$ by Eq. (3), respectively. To obtain the estimates of $P(F)$ and $P(F_i)$ ($i = 1, 2, \ldots, n$), a total of $n+1$ repeated SS runs are needed. This remains computationally demanding especially when n is large (e.g., for soil slopes) though SS significantly improves computational efficiency for a single rare failure event compared with direct MCS (e.g., Au and Beck, 2001; Wang et al., 2011; Singh et al., 2013c; Li et al., 2016c). This problem is resolved by GSS in the next subsection.

3.2. Generalized Subset Simulation algorithm

GSS generalizes SS to allow efficient estimation of the failure probabilities of multiple failure events simultaneously in a single simulation run. It was originally developed for structures by Li e al. (2015), where system failure was not considered and remained unexplored in the field of geotechnical reliability and risk.

The major difference between GSS and SS lies in determining intermediate failure events and selecting conditional "seed" samples during simulation. As discussed in Section 3.1, intermediate failure events $E^{(k)} = \{Y < y^{(k)}, k = 1, 2, \ldots, m\}$ in SS are determined using the driving variable Y (e.g., $Y = G_s$ for system failure event and $Y = G_i$ for i-th scenario failure event). Using different driving variables in SS, samples progressively populate different failure domains, yielding their corresponding failure probabilities. On the other hand, GSS

simultaneously drives samples to multiple failure domains through unified intermediate failure events for them.

Consider, for example, the system failure event F and n scenario failure events F_i, $i = 1$, $2, \ldots, n$, of slope stability. Let $U^{(k)}$, $k = 1, 2, \ldots, M$ denote the unified intermediate failure event at the k-th simulation level of GSS, where M is the number of simulation levels in GSS. In the context of GSS, $U^{(k)}$ is defined as the union of intermediate failure events of F and F_i, $i = 1, 2, \ldots, n$, which is written as:

$$U^{(k)} = F^{(k)} \bigcup F_1^{(k)} \bigcup F_2^{(k)} \bigcup \cdots \bigcup F_n^{(k)}$$
$$= \left\{G_s < y_s^{(k)}\right\} \bigcup \left\{G_1 < y_1^{(k)}\right\} \bigcup \left\{G_2 < y_2^{(k)}\right\} \bigcup \cdots \bigcup \left\{G_n < y_n^{(k)}\right\}, \quad k = 1, 2, \ldots, M \quad (4)$$

where $F^{(k)} = \left\{G_s < y_s^{(k)}\right\}$ and $F_i^{(k)} = \left\{G_i < y_i^{(k)}\right\}$, $i = 1, 2, \ldots, n$, are the intermediate failure events of F and F_i, respectively, at the k-th simulation level of GSS, and are defined by their respective intermediate threshold values $y_s^{(k)}$ and $y_i^{(k)}$. Similar to SS, $y_s^{(k)}$ and $y_i^{(k)}$, $i = 1, 2, \ldots, n$, are determined adaptively using information from simulated samples during GSS, as described below.

As shown in Figure 3, GSS starts with direct MCS, in which N MCS samples are generated. The G_s and G_i, $i = 1, 2, \ldots, n$, values of the N samples are calculated. The G_s values are then ranked in a descending order. The $(1-p_0)N$-th value in the descending list of G_s values is chosen as $y_s^{(1)}$ so that the sample estimate for $P(F^{(1)}) = P(G_s < y_s^{(1)})$ is always p_0. There are p_0N samples with $F^{(1)} = \{G_s < y_s^{(1)}\}$ among the samples generated by direct MCS. Similarly, $y_i^{(1)}$, $i = 1, 2, \ldots, n$, are determined, and p_0N samples with $F_i^{(1)} = \{G_i < y_i^{(1)}\}$ are selected for each scenario failure event. After that, $U^{(1)}$ is determined as the union of

$F^{(1)}$ and $F_i^{(1)}$, $i = 1, 2, \ldots, n$. The samples in $U^{(1)}$ are those satisfying $F^{(1)} = \{G_s < y_s^{(1)}\}$ or $F_i^{(1)} = \{G_i < y_i^{(1)}\}$ for any $i = 1, 2, \ldots, n$. Let N_1 denote the number of samples of $U^{(1)}$. The probability $P(U^{(1)})$ of $U^{(1)}$ is estimated as $P(U^{(1)}) \approx N_1/N$. The N_1 samples in $U^{(1)}$ are used as "seed" samples for MCMCS to simulate additional $N\text{-}N_1$ conditional samples in $U^{(1)}$. This results in N conditional samples in $U^{(1)}$, based on which $y_s^{(2)}$ and $y_i^{(2)}$, $i = 1$, $2, \ldots, n$, are determined so that the sample estimates of $P(F^{(2)}|U^{(1)})$ and $P(F_i^{(2)}|U^{(1)})$ are equal to p_0. Next, $U^{(2)}(F^{(2)} \bigcup F_1^{(2)} \bigcup F_2^{(2)} \bigcup \cdots \bigcup F_n^{(2)})$ is constructed, and N_2 samples in $U^{(2)}$ are identified as "seed" samples for MCMCS to generate conditional samples in the next simulation level. This procedure is repeatedly performed until all failure domains concerned or a desired failure probability level are reached. The samples provide estimates of $P(F)$ and $P(F_i)$, which is presented in the next subsection.

3.3. Calculating failure probabilities of slope system and scenario failure events

The failure probabilities of different failure events (e.g., F and F_i, $i = 1, 2, \ldots, n$) concerned might be different, and their failure domains are, therefore, reached at different simulation levels during GSS. As the number of simulation levels increases, the failure domains of failure events with relatively large failure probabilities are first arrived. For example, $P(F)$ is, in theory, greater than any $P(F_i)$ values since F is defined the union of F_i, $i = 1, 2, \ldots, n$ (see Eq. (1)). Hence, the failure domain of F is arrived with the least simulation levels. Let M_F denote the number of simulation levels needed to reach the failure domain of F. Then, $P(F)$ is calculated as:

$$P(F) = P(U^{(1)})P(U^{(2)}|U^{(1)})\cdots P(U^{(M_F-1)}|U^{(M_F-2)})P(F|U^{(M_F-1)}) = \prod_{k=1}^{M_F-1} \frac{N_k}{N} \times \frac{N_F}{N} \qquad (5)$$

where $P(U^{(k)}|U^{(k-1)})$, $k = 2, 3\ldots, M_F$-1, is conditional probability of $U^{(k)}$ given sampling

in $U^{(k-1)}$, and is calculated as the ratio of the number N_k of "seed" samples selected for the

k-th MCMCS level among N samples with $U^{(k-1)}$ over N; $P(F|U^{(M_F-1)})$ is the conditional

probability of F given sampling in $U^{(M_F-1)}$, and is estimated as the ratio of the number N_F

of system failure samples among N samples generated in $U^{(M_F-1)}$ over N. After the failure

domain of a particular failure event (e.g., F and F_i) is reached, its intermediate failure event

is dropped from the unified intermediate failure event in subsequent simulation levels,

because there are already enough samples for investigating the failure event. As simulation

level k increases, the failure events (e.g., F and F_i) reach their respective target failure

domains progressively, and the number of failure events involved in the unified

intermediate failure event decreases. Let M_i denote the number of simulation levels needed

to reach the failure domain of F_i. Then, $P(F_i)$ is calculated as:

$$P(F_i) = P(U^{(1)})P(U^{(2)}|U^{(1)})\cdots P(U^{(M_i-1)}|U^{(M_i-2)})P(F_i|U^{(M_i-1)}) = \prod_{k=1}^{M_i-1} \frac{N_k}{N} \times \frac{N_{F,i}}{N} \qquad (6)$$

where $P(F_i|U^{(M_i-1)})$ is conditional probability of F_i given sampling in $U^{(M_i-1)}$, and is

estimated as the ratio of the number $N_{F,i}$ of failure samples belonging to F_i among N

samples generated in $U^{(M_i-1)}$ over N.

GSS can proceed until all the failure domains of failure events (e.g., F and F_i)

concerned are reached, providing estimates of $P(F)$ and $P(F_i)$, $i = 1, 2, \ldots, n$, by a single run

of simulation. Note that $P(F_i)$ values of some scenario failure events might be extremely small (e.g., less than 10^{-5}) and so they contribute very little to slope system failure. In practice, these scenario failure events with extremely small $P(F_i)$ values can be ignored. Hence, GSS can also be stopped when the simulation reaches a failure probability level (e.g., $P(F_i) < P(F)/100$ or 10^{-5}) pre-defined by users, resulting in estimates of $P(F)$ and $P(F_i)$ values greater than the pre-defined failure probability level. This leads to a further saving in computational costs.

4. Identification of key failure events based on GSS results

Although there can be a large number of slope scenario failure events, many of them are correlated, and slope system failure can be attributed to only a few RFEs that are relatively independent (e.g., Zhang et al. 2011, 2012; Li et al. 2013, 2014). This section applies probabilistic network evaluation technique (PNET) (Ang et al, 1975; Ang and Tang, 1984) to identify RFEs and key failure events of slope stability from scenario failure events based on GSS results.

Figure 4 shows the implementation procedure of PNET schematically. Let n_p denote the number of scenario failure events, the $P(F_i)$ values of which are obtained from a single GSS run. Herein, $n_p \leq n$, depending on when GSS is stopped. These n_p scenario failure events collectively form a failure event library (FEL). In the FEL, the scenario failure event with the largest $P(F_i)$ value is taken as the first RFE, denoted by $F_{r,1}$. Conventional statistical analysis (e.g., Ang and Tang, 2007) is then performed to estimate the Pearson correlation

coefficients (PCCs) between LSF (or safety factor) of $F_{r,1}$ and that of the remaining scenario failure events based on N direct MCS random samples generated in the first level of GSS. The scenario failure events with PCCs greater than a threshold value ρ_d (e.g., 0.8~0.9) are "represented" by $F_{r,1}$ and are excluded from the FEL. The procedure described above is repeated until the FEL contains no failure events, resulting in a number n_r of RFEs (i.e., $F_{r,i}$, $i = 1, 2, …, n_r$), which are considered as relatively independent (Ang and Tang, 1984). The relative contribution RC_i of $F_{r,i}$ to slope system failure is calculated as:

$$RC_i = P(F_{r,i}) / P(F), i = 1, 2, …, n_r \tag{7}$$

where $P(F_{r,i})$ = the failure probability of the i-th RFE, and it has been obtained during GSS. As indicated by Eq. (7), the contribution of $F_{r,i}$ to slope system failure increases as RC_i increases. Scenario failure events with relatively large RC_i values, e.g., greater than 1% (Neves et al., 2008; Kim et al., 2013), are considered as key failure events.

PNET has several successful applications in slope system reliability analysis (e.g., Zhang et al. 2011, 2012; Li et al. 2013, 2014). These existing studies used PNET to select RFEs for evaluating $P(F)$, where $P(F_i)$ values are approximately calculated using simplified reliability methods (e.g., First order second moment method or FORM) and the accuracy of $P(F)$ depends on the selected RFEs. This study uses PNET to select RFEs and key failure events for making risk-informed design decisions and remedial measure of slopes using the estimates of $P(F)$ and $P(F_i)$ from GSS. The accuracy of $P(F)$ obtained from the proposed approach is not affected by RFEs. This allows checking whether or not the number of RFEs

selected by PNET is sufficient to represent the slope system. A sufficient number of RFEs shall ensure that the summation of RC_i, $i = 1, 2, \ldots, n_r$, is close to or greater than unity or, equivalently, the summation of $P(F_{r,i})$, $i = 1, 2, \ldots, n_r$, is virtually identical to or greater than $P(F)$. Note that the summation of $P(F_{r,i})$ can exceed $P(F)$ because the RFEs selected by PNET might be correlated, depending on the adopted ρ_d value.

5.   A Soil Slope Example

The proposed approach is applied to evaluating the system failure probability of a two-layered soil slope shown in Figure 5(a) and to identifying its key failure events. This example was considered to explore slope system reliability problems in literature, e.g., Ching et al. (2009), Low et al. (2011), Ji and Low (2012), and Kang et al. (2015). As shown in Figure 5(a), the slope has a height of 24.0m and a slope angle of about 37.0°, and it comprises two soil layers. In this example, the safety factor of slope stability under undrained condition is calculated using Bishop's simplified method. The geo-mechanical parameters needed in the calculation include the undrained shear strength (c_{u1} and c_{u2}) and unit weight of the two soil layers. To enable a consistent comparison with results reported in literature, the soil properties used in this study are taken as those adopted in previous studies. c_{u1} and c_{u2} are lognormally distributed with respective mean values of 120 and 160kPa and respective standard deviations of 36 and 48kPa, indicating that c_{u1} and c_{u2} have a coefficient of variation (COV) of 0.3. The unit weights of the two soil layers are taken as a deterministic value of 19kN/m^3..

Figure 5(a) shows 6142 potential slip surfaces of the soil slope, each of which is considered as a possible failure scenario. Correspondingly, the slope system failure event F is the union of these 6142 scenario failure events F_i, $i = 1, 2, \ldots, 6142$ (see Figure 5(b)). The LSF of F_i is defined as $G_i = FS_i - 1$, where FS_i is safety factor of the i-th slip surface for a given set of soil properties. The LSF of F is $G_s = \min\{G_i, i = 1, 2, \ldots, 6142\}$, or, equivalently, $G_s = FS_{min} - 1$, where $FS_{min} = \min\{FS_i, i = 1, 2, \ldots, 6142\}$. The FS_i and FS_{min} values are calculated using Bishop's simplified method in MATLAB (e.g., Duncan and Wright, 2005). For reference, at the mean values of c_{u1} and c_{u2}, FS_{min} is calculated as 1.990 in this study, which agrees well with the value 1.993 estimated in SLOPE/W and those reported in literature (e.g., 1.992 by Cho (2013) and 1.993 by Kang et al. (2015)).

A GSS run with $N = 500$ and $p_0 = 0.1$ is performed to calculate $P(F)$ and $P(F_i)$ of different failure events. The simulation run is performed until all the failure domains of F_i with $P(F_i)$ values greater than $P(F)/100$ are reached, yielding estimates of $P(F)$ and $P(F_i)$ of 2960 failure events, i.e., $n_p = 2960$ in this example. Although the GSS run is stopped when the failure probability level less than $P(F)/100$ is reached in this example, it can also be stopped until failure probabilities of all the failure events are obtained, if needed. This is further illustrated using a rock slope example in the next section.

5.1. Reliability analysis results of the soil slope

Table 1 summarizes the procedure of the GSS run in this example, which consists of 8 simulation levels, including a direct MCS level (i.e, $k = 0$) and 7 MCMCS levels (i.e., $k = 1$,

2, …, 7). The GSS run reaches the failure domain of F at $k = 3$ (i.e., the 3rd MCMCS level) by generating a total of 500+397+384+362 = 1643 random samples (see Column 3 of Table 1). Based on these 1643 random samples, $P(F)$ is estimated as 4.4×10^{-3} by Eq. (5). As shown in Table 2, the estimate of $P(F)$ obtained from GSS agrees well those obtained using direct MCS and bound methods based on FORM in literature. This validates the $P(F)$ estimate obtained from the proposed approach. In addition, as shown in Column 5 of Table 2, the number (i.e., 1643) of random samples generated in GSS is much less than those (i.e., 1.0×10^4 and 2.0×10^4) used in direct MCS. More importantly, although the direct MCS run with 1.0×10^4 or 2.0×10^4 samples is able to generate reasonably accurate estimate of $P(F)$ in this example, such number of samples may not be sufficient to calculate $P(F_i)$ values of some scenario failure events that are smaller, as discussed below.

As shown in Table 1, the GSS run also arrives at failure domains of 90, 829, 821, 716, and 504 scenario failure events at $k = 3$, 4, 5, 6, and 7, respectively. This provides $P(F_i)$ values of 2960 potential slip surfaces by the single run of simulation, avoiding repeated simulation runs (e.g., SS) for each slip surface. Figure 6 shows the 2960 potential slip surfaces, the $P(F_i)$ values of which vary from 1.8×10^{-5} to 2.6×10^{-3}. As shown in Figure 6, the scenario failure event with the largest and smallest $P(F_i)$ values are plotted with a red dotted line and a black dashed line, respectively. The scenario failure event with the largest $P(F_i)$ value (i.e., 2.6×10^{-3}) is referred to as "probabilistic critical slip surface". Its failure domain and slope system failure domain are reached simultaneously at $k = 3$. The smallest $P(F_i)$ (i.e., 1.8×10^{-5}) value is obtained at the 7th MCMCS level, where failure domains of

17

504 scenario failure events are reached simultaneously (see Table 1). It is noted that the

smallest $P(F_i)$ (i.e., 1.8×10^{-5}) value at the 7th MCMCS level is already less than $P(F)/100$.

The GSS run is then stopped at $k = 7$ according to the pre-defined stopping criterion,

resulting in a total of 2963 random samples (i.e., sum over Column 3 of Table 1). Consider

using a direct MCS run to estimate of $P(F)$ value and $P(F_i)$ values of the 2960 scenario

failure events shown in Figure 6. The number of random samples needed in direct MCS is

controlled by the minimum $P(F_i)$ value (i.e., 1.8×10^{-5}). As a rule of thumb (e.g., Ang and

Tang, 2007), about 5.6×10^5 (i.e., $10/1.8 \times 10^{-5}$) random samples are required in direct MCS,

which is about two orders of magnitude greater than that of random samples generated by

GSS in this example. Compared with direct MCS, the proposed approach significantly

improves the computational efficiency of evaluating $P(F)$ and $P(F_i)$ of slope stability,

particularly at relatively small probability levels.

5.2. *Identification of representative and key failure events of the soil slope*

This section applies PNET described in Section 4 to identify RFEs from 2960 scenario

failure events, whose $P(F_i)$ values were obtained from the single GSS run in the last

subsection. In PNET, the value of ρ_d is taken as 0.8 (Ma and Ang, 1981; Ang and Tang,

1984). It is found that the 2960 scenario failure events are represented by two RFEs, as

shown in Figure 7 by a dotted line with circles and a solid line with diamonds. The 1st RFE

is located at the top soil layer of the slope. It is identical to the probabilistic critical slip

surface shown in Figure 6 and has a $P(F_{r,1})$ value of 2.6×10^{-3}. The 2nd RFE goes through

two soil layers and its $P(F_{r,2})$ value is 1.7×10^{-3}. The two RFEs selected in this study are similar to those adopted to evaluate system reliability of this soil slope in previous studies (e.g., Low et al., 2011; Ji and Low, 2012; Cho, 2013). In addition, the $P(F_{r,i})$ values of the two RFEs obtained from the single GSS run agree well with those reported in literature (see Columns 3 and 4 in Table 2), which further validates the proposed approach.

The values of RC_1 and RC_2 for the two RFEs are evaluated as 59% and 39% using Eq. (7), respectively. The summation of RC_1 and RC_2 is close to unity, indicating that the two RFEs in Figure 7 represent well the soil slope system. Since RC_1 and RC_2 are relatively large, both RFEs are considered as key failure events. This information is valuable in making design decisions and remedial measures of soils slopes, where a large number of scenario failure events usually exist. It is also worth noting that the RFEs are not necessarily key failure events for some slopes. This will be further illustrated using a rock slope example in the next section.

5.3. Comparison with results from original SS

For comparison, SS runs are also performed to calculate $P(F)$ and $P(F_{r,i})$. For each failure event (e.g., F, $F_{r,1}$ and $F_{r,2}$), the driving variable in SS is defined using its corresponding LSF. Thirty independent SS runs with $N = 500$ and $p_0 = 0.1$ are performed to obtain 30 estimates of failure probability of the failure event. A total of 90 SS runs are performed to generate 30 estimates of $P(F)$, $P(F_{r,1})$, and $P(F_{r,2})$. Note that only 30 independent GSS runs with $N = 500$ and $p_0 = 0.1$ are needed to generate 30 estimates of $P(F)$, $P(F_{r,1})$, and $P(F_{r,2})$.

Table 3 summarizes the sample average values and COVs of $P(F)$, $P(F_{r,1})$, and $P(F_{r,2})$. The average values of $P(F)$, $P(F_{r,1})$, and $P(F_{r,2})$ obtained from SS agree well with those of GSS, demonstrating their unbiased nature. Table 3 also summarizes the average numbers N_T of samples generated in SS and GSS runs for estimating $P(F)$, $P(F_{r,1})$, and $P(F_{r,2})$. To account for the effect of the number of samples on the variability of failure probability estimates, the unit COV, defined as $\text{COV} \times \sqrt{N_T}$ (Au and Beck, 2003b; and Au 2007), is applied as a measure of the computational efficiency. As shown in Column 5 of Table 3, the unit COV values of the GSS estimates for $P(F)$, $P(F_{r,1})$, and $P(F_{r,2})$ are slightly smaller than those using SS. This indicates that GSS requires slightly less computational efforts than SS to achieve the same computational accuracy for evaluating $P(F)$, $P(F_{r,1})$, and $P(F_{r,2})$ in this example. More importantly, using SS to estimate the occurrence probabilities of slope system failure event and different scenario failure events (e.g., $F_{r,1}$ and $F_{r,2}$) needs to repeatedly perform simulations, which might be a laborious task, particularly when the number of failure events concerned is relatively large (e.g., 2960 scenario failure events shown in Figure 7). This problem is successfully resolved by GSS in this study.

6. A Rock Slope Example

For further illustration, this section applies the proposed approach to evaluate the system reliability of a rock slope. The example was considered to explore system effects on reliability analysis of rock slope stability by Low (1997), Jimenez-Rodriguez and Sitar (2007), and Li et al. (2009). Figure 8 shows a tetrahedral wedge formed by two intersecting discontinuity planes (i.e., planes 1 (B'DO) and 2 (B'CO)) in the rock slope and explains the

geometry parameters involved in the example. For system reliability analysis of the rock slope, 10 uncertain parameters are considered, and they are modeled by uncorrelated normal random variables, the statistics of which are adopted from Low (1997), as shown in Table 4.

Four scenario failure events (including sliding on both planes F_1, sliding along plane 1 only F_2, sliding along plane 2 only F_3, and floating failure F_4) are considered in this example (e.g., Low, 1997). As shown in Figure 9, the occurrence of any ones among F_1-F_4 leads to the slope failure F, and F_1-F_4 are represented as intersections of different components. Table 5 gives LSFs (i.e., G_1-G_4 and g_1-g_9) of F_1-F_4 and their components. The LSF of F is defined as $G = \min\{G_1, G_2, G_3, G_4\}$. Further details are referred to Low (1997) and Li et al. (2009).

6.1. Reliability analysis results of the rock slope

A GSS run with $N = 500$, $p_0 = 0.1$, and 12 simulation levels (including a direct MCS level at $k = 0$ and 11 MCMCS levels at $k = 1, 2, \ldots, 11$) is performed to calculate $P(F)$ and $P(F_i)$, $i = 1, 2, 3, 4$. The simulation is stopped until all the failure domains of F_1- F_4 are reached. Table 6 summarizes the procedure of the GSS run in this example. The GSS run reaches failure domains of F and F_2 at $k = 1$ by generating 500+383 = 883 random samples (see Column 3 of Table 6), which yields $P(F)$ and $P(F_2)$ estimates of 8.2×10^{-2} and 6.7×10^{-2}, respectively. The simulation proceeds to approach failure domains of F_1, F_4, and F_3 progressively. Their failure probabilities are estimated as $P(F_1) = 1.6 \times 10^{-2}$, $P(F_4) = 6.26 \times 10^{-6}$, and $P(F_3) = 1.42 \times 10^{-10}$ at $k = 2, 6$, and 11, based on 1258, 2902, and 5152 samples, respectively. As shown in Table 7, the estimates of $P(F)$, $P(F_1)$, $P(F_2)$, and $P(F_4)$ obtained from a single GSS run agree well with those reported by Low (1997) using direct MCS with 1600,000 samples and bound method based on FORM. However, the $P(F_3)$ value from GSS is about three orders

21

of magnitude less than that (i.e., 6.25×10^{-7}) from direct MCS with 1600,000 samples. Note that only one failure sample for F_3 is obtained among 1600,000 samples from direct MCS in Low (1997), the number of which is not sufficient to accurately estimate $P(F_3)$.

For further validation, a direct MCS run with 10^{12} samples is performed to evaluate $P(F_3)$ in this study. The resulting $P(F_3)$ value is 3.55×10^{-10}, and its corresponding unit COV is calculated as 5310. In addition, 30 independent GSS runs are also performed to obtain 30 estimates of $P(F)$ and $P(F_i)$, $i = 1, 2, 3, 4$, each of which, on average, generates a total of 5262 random samples. Based on the 30 estimates of $P(F_3)$ from GSS, its average is estimated as 2.55×10^{-10}, which is favorably comparable with that from direct MCS with 10^{12} samples, and has a unit COV of 103 that is about 1/52 of that for direct MCS. This means that the computational effort needed to calculate $P(F_3)$ in the proposed approach is about 1/2704 of that used for direct MCS to achieve the same computational accuracy. Compared with direct MCS, the proposed approach significantly reduces the computational effort at small probability levels.

6.2. Identification of representative and key failure events of the rock slope

Although only four scenario failure events are considered in the rock slope example, its RFEs are determined using PNET in this section to illustrate the difference between RFEs and the key failure events. Based on random samples generated in the GSS run, the correlation coefficients among the LSFs of the four scenario failure events are calculated and showed in Table 8. The values are all less than 0.8. Taking $\rho_d = 0.8$ in the criterion for

PNET, all the four scenario failure events are selected as RFEs. Specifically, F_2, F_1, F_4, and F_3 are selected as $F_{r,1}$, $F_{r,2}$, $F_{r,3}$, and $F_{r,4}$, respectively. The respective RC_i values of $F_{r,i}$, $i = 1$, 2, 3, 4 are calculated to be 8.17×10^{-1}, 1.95×10^{-1}, 7.63×10^{-5}, and 1.73×10^{-9} using Eq. (7) and $P(F_i)$ values from GSS (see Table 7). It is obvious that F_1 and F_2 have much more contribution to slope system failure than F_3 and F_4. The scenario failure events F_1 (sliding along both planes) and F_2 (sliding along plane 1 only) are thus taken as the key failure events among the four RFEs. This illustrates that the RFEs selected by PNET are not necessarily the key failure events. As an application of this finding to slope design, scenario failure event F_2 is expected to govern design. Design measures shall be applied to prevent the rock wedge from sliding along plane 1, since the relative contribution of F_2 (i.e., $F_{r,1}$) to slope failure is more than 80%.

7. Conclusions

This paper presented an efficient computer-based simulation method to evaluate the system failure probability $P(F)$ of slope stability and to identify key failure events with significant contributions to slope failure. The proposed approach was illustrated using a soil slope example with a large number of scenario failure events and a rock slope example with only four scenario failure events. Major conclusions drawn from this study are given below:

(1) The proposed approach provides proper estimates of $P(F)$ and $P(F_i)$ by a single GSS run. This avoids repeatedly performing simulations (e.g., SS) for different failure events (e.g., F and F_i, $i = 1, 2, …, n$), which can be time consuming when the number of scenario

failure events is large (e.g., for soil slopes).

(2) Compared with direct MCS, the proposed approach significantly improves the computational efficiency of calculating $P(F)$ and $P(F_i)$, particularly for failure events with small failure probabilities. The accuracy of $P(F)$ estimated from the proposed approach does not rely on the selection of representative failure events (RFEs), because $P(F)$ is obtained through GSS before RFEs are determined. This allows determining the number of RFEs to represent the slope system in a rational manner.

(3) Using the proposed approach, the key failure events of slope stability are rationally determined based on their relative contributions to slope system failure, which provides useful insights for making slope design decisions and remedial measures.

References

Ang, A. H-S., Chaker, A. A., and Abdelnour, J. (1975). Analysis of activity networks under uncertainty. Journal of the Engineering Mechanics Division, 101(4), 373-387.

Ang, A. H-S., and Tang, W. H. (2007) Probability concepts in engineering: emphasis on applications to civil and environmental engineering (2nd edition), Hoboken, New Jersey: John Wiley & Sons, Inc.

Ang, A. H-S., and Tang, W. H. (1984). Probability Concepts in Engineering Planning and Design: Design, Risk and Reliability, vol. 2. New York, Wiley.

Au, S. K. (2007). Augmenting approximate solutions for consistent reliability analysis. Probabilistic Engineering Mechanics, 22(1), 77-87.

Au, S. K., and Beck, J. L. (2003a). Subset simulation and its application to seismic risk based on dynamic analysis. Journal of Engineering Mechanics, 129(8), 901-917.

Au, S. K., and Beck, J. L. (2003b). Important sampling in high dimensions. Structural safety, 25(2), 139-163.

Au, S. K., and Beck, J. L. (2001). Estimation of small failure probabilities in high dimensions by subset simulation. Probabilistic Engineering Mechanics, 16(4), 263-277.

Au, S. K., and Wang, Y. (2014). Engineering risk assessment with subset simulation. Singapore, John Wiley & Sons Singapore Pte. Ltd.

Baecher, G. B., and Christian, J. T. (2003). Reliability and statistics in geotechnical engineering. John Wiley & Sons Ltd.

Cao, Z. J, Wang, Y., and Li, D. Q. (2016). Quantification of prior knowledge in geotechnical site characterization. Engineering Geology, 203,107–116.

Ching, J., Phoon, K. K., and Hu, Y. G. (2009). Efficient evaluation of reliability for slopes with circular slip surfaces using importance sampling. Journal of Geotechnical and Geoenvironmental Engineering, 135(6), 768-777.

Cho, S. E. (2013). First-order reliability analysis of slope considering multiple failure modes. Engineering Geology, 154, 98-105.

Chowdhury, R. N., and Xu, D. W. (1995). Geotechnical system reliability of slopes. Reliability Engineering & System Safety, 47(3), 141-151.

Christian, J. T., Ladd, C. C., and Baecher, G. B. (1994). Reliability applied to slope stability analysis. Journal of Geotechnical Engineering, 120(12), 2180-2207.

Duncan, J. M., and Wright, S. G. (2005). Soil Strength and Slope Stability. Hoboken, New Jersey: John Wiley & Sons, Inc.,

El-Ramly, H., Morgenstern, N. R., and Cruden, D. M. (2005). Probabilistic assessment of stability of a cut slope in residual soil. Geotechnique, 55(1), 77–84.

Huang, J., Griffiths, D. V., and Fenton, G. A. (2010). System reliability of slopes by RFEM. Soils and Foundations, 50(3), 343-353.

GEO-SLOPE International Ltd. (2015). GeoStudio 2012, http://www.geo-slope.com/.

Kang, F., Han, S., Salgado, R., and Li, J. (2015). System probabilistic stability analysis of soil slopes using Gaussian process regression with Latin hypercube sampling. Computers and Geotechnics, 63, 13-25.

Kang, F, Xu Q., Li, J. (2016). Slope reliability analysis using surrogate models via new support vector machines with swarm intelligence, Applied Mathematical Modelling, doi: 10.1016/j.apm.2016.01.050.

Kainthola, A., Singh, P. K., and Singh, T. N. (2015). Stability investigation of road cut slope in basaltic rockmass, Mahabaleshwar, India. Geoscience Frontiers, 6(6), 837-845.

Kim, D. S., Ok, S. Y., Song, J., and Koh, H. M. (2013). System reliability analysis using dominant failure modes identified by selective searching technique. Reliability Engineering & System Safety, 119, 316-331.

Ji, J., and Low, B. K. (2012). Stratified response surfaces for system probabilistic evaluation of slopes. Journal of Geotechnical and Geoenvironmental Engineering, 138(11), 1398-1406.

Jiang, S. H., Li, D. Q., Cao, Z. J., Zhou, C. B., and Phoon, K. K. (2015). Efficient system reliability analysis of slope stability in spatially variable soils using Monte Carlo simulation. Journal of Geotechnical and Geoenvironmental Engineering, 141(2), 04014096.

Jimenez-Rodriguez, R., and Sitar, N. (2007). Rock wedge stability analysis using system reliability methods. Rock Mechanics and Rock Engineering, 40(4), 419-427.

Jimenez-Rodriguez, R., Sitar, N., and Chacon, J. (2006). System reliability approach to rock slope stability. International Journal of Rock Mechanics and Mining Sciences, 43(6), 847-859.

Li, H. S. (2011). Subset simulation for unconstrained global optimization. Applied

Mathematical Modelling, 35(10), 5108-5120.

Li, H. S., Ma, Y. Z., and Cao, Z. (2015). A generalized Subset Simulation approach for estimating small failure probabilities of multiple stochastic responses. Computers & Structures, 153, 239-251.

Li, L., Wang, Y., and Cao, Z. (2014). Probabilistic slope stability analysis by risk aggregation. Engineering Geology, 176, 57-65.

Li, L., Wang, Y., Cao, Z., and Chu, X. (2013). Risk de-aggregation and system reliability analysis of slope stability using representative slip surfaces. Computers and Geotechnics, 53, 95-105.

Li, D. Q., Jiang, S. H., Chen, Y. F., and Zhou, C. B. (2011a). System reliability analysis of rock slope stability involving correlated failure modes. KSCE Journal of Civil Engineering, 15(8), 1349-1359.

Li, D.Q., Chen, Y.F., Lu, W.B., and Zhou, C.B. (2011b). Stochastic response surface method for reliability analysis of rock slopes involving correlated non-normal variables. Computers and Geotechnics, 38(1), 58-68.

Li, D. Q., Qi, X. H., Cao, Z. J, Phoon, K. K., and Zhou, C. B. (2016a). Evaluating slope stability uncertainty using coupled Markov chain. Computers and Geotechnics, 73, 72–82.

Li, D. Q., Xiao, T., Cao, Z. J., Phoon, K. K., and Zhou, C. B. (2016b). Efficient and consistent reliability analysis of soil slope stability using both limit equilibrium analysis and finite element analysis. Applied Mathematical Modelling, 40(9–10),

5216–5229.

Li, D. Q., Xiao, T., Cao, Z. J., Zhou, C. B., and Zhang, L. M. (2016c). Enhancement of random finite element method in reliability analysis and risk assessment of soil slopes using Subset Simulation. Landslides, 13, 293–303.

Li, D. Q., Zheng, D., Cao, Z. J., Tang, X. S., and Phoon, K. K. (2016d). Response surface methods for slope reliability analysis: Review and comparison. Engineering Geology, 203, 3–14.

Li, D. Q., Zhou, C. B., Lu, W. B., and Jiang, Q. H. (2009). A system reliability approach for evaluating stability of rock wedges with correlated failure modes. Computers and Geotechnics, 36(8), 1298-1307.

Low, B. K. (1997). Reliability analysis of rock wedges. Journal of Geotechnical and Geoenvironmental Engineering, 123(6), 498-505.

Low, B. K., Zhang, J., and Tang, W. H. (2011). Efficient system reliability analysis illustrated for a retaining wall and a soil slope. Computers and Geotechnics, 38(2), 196-204.

Ma, H. F., and Ang, A. S. (1981). Reliability analysis of redundant ductile structural systems. University of Illinois Engineering Experiment Station. College of Engineering. University of Illinois at Urbana-Champaign.

Mathworks, Inc., MATLAB - the language of technical computing, (2015) http://www.mathworks.com/products/matlab/.

Neves, R. A., Mohamed-Chateauneuf, A., and Venturini, W. S. (2008). Component and

system reliability analysis of nonlinear reinforced concrete grids with multiple failure modes. Structural Safety, 30(3), 183-199.

Oka, Y., and Wu, T. H. (1990). System reliability of slope stability. Journal of Geotechnical Engineering, 116(8), 1185-1189.

Santoso, A. M., Phoon, K. K., and Quek, S. T. (2011). Modified Metropolis–Hastings algorithm with reduced chain correlation for efficient subset simulation. Probabilistic Engineering Mechanics, 26(2), 331-341.

Sinha, S., Singh, T. N., Singh, V. K., and Verma, A. K. (2010). Epoch determination for neural network by self-organized map (SOM). Computational Geosciences, 14(1), 199-206.

Singh, P. K., Wasnik, A. B., Kainthola, A., Sazid, M., and Singh, T. N. (2013a). The stability of road cut cliff face along SH-121: a case study. Natural hazards, 68(2), 497-507.

Singh, T. N., Ahmad, M., Kainthola, A., Singh, R., and Kumar, S. (2013b). A stability assessment of a hill slope—an analytical and numerical approach. International Journal of Earth Sciences and Engineering, 6(1), 50-60.

Singh, R., Umrao, R. K., Singh, T. N. (2013c). Probabilistic analysis of slope in Amiyan landslide area, Uttarakhand Geomatics. Natural Hazards and Risk, 4 (1), 13-29.

Singh, A. K., Kainthola, A., and Singh, T. N. (2012). Prediction of factor of safety of a slope with an advanced friction model. International Journal of Rock Mechanics and Mining Sciences, 55, 164-167.

Tang, X.S., Li, D.Q., Zhou, C.B., and Phoon, K.K. (2015). Copula-based approaches for

evaluating slope reliability under incomplete probability information. Structural Safety, 52, 90-99.

Wang, Y., Cao, Z., and Au, S. K. (2011). Practical reliability analysis of slope stability by advanced Monte Carlo simulations in a spreadsheet. Canadian Geotechnical Journal, 48(1), 162-172.

Wang, Y., Cao, Z. J., and Au, S. K. (2010). Efficient Monte Carlo simulation of parameter sensitivity in probabilistic slope stability analysis. Computers and Geotechnics, 37(7), 1015-1022.

Wang, Y., Cao, Z. J, and Li, D. Q. (2016). Bayesian perspective on geotechnical variability and site characterization. Engineering Geology, 203, 117–125.

Zeng, P., and Jimenez, R. (2014). An approximation to the reliability of series geotechnical systems using a linearization approach. Computers and Geotechnics, 62, 304-309.

Zhang, J., Huang, H. W., Juang, C. H., and Li, D. Q. (2013). Extension of Hassan and Wolff method for system reliability analysis of soil slopes. Engineering Geology, 160, 81-88.

Zhang, J., Huang, H. W., and Phoon, K. K. (2012). Application of the Kriging-based response surface method to the system reliability of soil slopes. Journal of Geotechnical and Geoenvironmental Engineering, 139(4), 651-655.

Zhang, J., Zhang, L. M., and Tang, W. H. (2011). New methods for system reliability analysis of soil slopes. Canadian Geotechnical Journal, 48(7), 1138-1148.

List of Tables:

Table 1. Summary of GSS procedure in the soil slope example

Simulation level, k	Number of "seed" samples, N_k	Number of samples generated in the k-th level , $N\text{-}N_k$	Conditional probability, $P(U^{(k+1)}|U^{(k)})^a$	Number of failure events occurring in the k-th simulation level
0	-	500	0.206	0
1	103	397	0.232	0
2	116	384	0.276	0
3	138	362	0.312	91 (including system failure)
4	156	344	0.332	829
5	166	334	0.348	821
6	174	326	0.368	716
7	184	316	0.332	504

Note a: $P(U^{(k+1)}|U^{(k)})$ is simplified as $P(U^{(1)})$ for k =0.

Table 2. Comparison of reliability analysis results of the soil slope example from different methods

Method	$P(F)$	$P(F_i)$ of the 1st RFE	$P(F_i)$ of the 2nd RFE	Number of samples	Sources
GSS	4.4×10^{-3}	2.6×10^{-3}	1.7×10^{-3}	1643	This study
Direct MCS	4.4×10^{-3}	-	-	1.0×10^{4}	Ching et al. (2009)
	4.05×10^{-3}	-	-	2.0×10^{4}	Ji and Low (2012)
	4.15×10^{-3}	-	-	2.0×10^{4}	Cho (2013)
Bound methods based on FORM	$4.32 \times 10^{-3}\text{-}4.41 \times 10^{-3}$	2.6×10^{-3}	1.9×10^{-3}	-	Low et al. (2011)
	$4.02 \times 10^{-3}\text{-}4.11 \times 10^{-3}$	2.6×10^{-3}	1.6×10^{-3}	-	Ji and Low (2012)
	$4.31 \times 10^{-3}\text{-}4.39 \times 10^{-3}$	2.6×10^{-3}	1.9×10^{-3}	-	Cho (2013)

Table 3. Comparison of soil slope reliability analysis results from different methods

Failure event	Failure probability		COV (%)		Average number of samples based on 30 simulation runs, N_T		Unit COV	
	SS	GSS	SS	GSS	SS	GSS	SS	GSS
1st RFE	2.5×10^{-3}	2.6×10^{-3}	57.8	38.6	1490	1697	22.3	15.9
2nd RFE	1.5×10^{-3}	1.6×10^{-3}	59.3	46.9	1535	1775	23.2	19.7
System failure	4.0×10^{-3}	4.2×10^{-3}	34.3	28.5	1400	1528	12.8	11.1

Note: results from 30 independent runs

Table 4. Summary of statistics of uncertain parameters (After Low (1997))

Uncertain parameters	Mean	Standard deviation	Distribution type
Normalized cohesions, $c_1/\gamma h$ and $c_2/\gamma h$	0.1	0.02	Normal
Tangent of friction angles, $\tan\phi_1$ and $\tan\phi_2$	0.7	0.15	Normal
Dip of discontinuity plane 1 (B'DO), δ_1	50	2.00	Normal
Dip of discontinuity plane 2 (B'DO), δ_2	48	2.00	Normal
Angle of BDC, θ_1	62	3.00	Normal
Angle of BCD, θ_2	20	3.00	Normal
Normalized water pressure parameters, $G_{w,1}$ and $G_{w,2}$	0.5	0.12	Normal

Table 5. Limit state functions for scenario failure events and their components (After Li et al. (2009))

Limit state function	Interpretation	Eq.
$G_1 = \max(g_1, -g_2, -g_3, g_8, g_9)$	Sliding on both planes, F_1	(8)
$G_2 = \max(g_3, g_4, -g_5, g_8, g_9)$	Sliding along plane 1 only, F_2	(9)
$G_3 = \max(g_2, g_6, -g_7, g_8, g_9)$	Sliding along plane 2 only, F_3	(10)
$G_4 = \max(g_5, g_7, g_8, g_9)$	Floating failure, F_4	(11)
$g_1 = FS - 1$	Wedge slides on both planes	(12)
$g_2 = a_1 - \dfrac{b_1 G_{w1}}{s_\gamma}$	Wedge contact on plane 2	(13)
$g_3 = a_2 - \dfrac{b_2 G_{w2}}{s_\gamma}$	Wedge contact on plane 1	(14)
$g_4 = FS_1 - 1$	Wedge slides only along plane 1	(15)
$g_5 = \left(a_1 - \dfrac{b_1 G_{w1}}{s_\gamma}\right) - \left(\dfrac{b_2 G_{w2}}{s_\gamma} - a_2\right)Z$	Wedge floating condition on plane 2	(16)
$g_6 = FS_2 - 1$	Wedge slides only along plane 2	(17)
$g_7 = \left(a_2 - \dfrac{b_2 G_{w2}}{s_\gamma}\right) - \left(\dfrac{b_1 G_{w1}}{s_\gamma} - a_1\right)Z$	Wedge floating condition on plane 1	(18)
$g_8 = \Omega - \varepsilon$	Kinematic admissibility	(19)
$g_9 = \varepsilon - \alpha$	Kinematic admissibility	(20)

Note: Interested readers are referred to Low (1997) and Li et al. (2009) for more details on these limit state functions and symbols involved in them.

Table 6. Summary of GSS procedure in the rock slope example

Simulation level, k	Number of "seed" samples, N_k	Number of samples generated in the k-th level, $N-N_k$	Conditional probability, $P(U^{(k+1)}\|U^{(k)})^a$	Failure probabilities obtained in the k-th level
0	-	500	0.234	-
1	117	383	0.250	$P(F) = 8.2\times10^{-2}$ $P(F_2)= 6.7\times10^{-2}$
2	125	375	0.154	$P(F_1)= 1.6\times10^{-2}$
3	77	423	0.180	-
4	90	410	0.188	-
5	94	406	0.190	-
6	95	405	0.100	$P(F_4) = 6.26\times10^{-6}$
7	50	450	0.100	-
8	50	450	0.100	-
9	50	450	0.100	-
10	50	450	0.100	-
11	50	450	0.100	$P(F_3) = 1.42\times10^{-10}$

Note a: $P(U^{(k+1)}|U^{(k)})$ is simplified as $P(U^{(1)})$ for $k =0$.

Table 7. Comparison of results obtained from GSS with those reported by Low (1997).

Method	$P(F)$	$P(F_1)$	$P(F_2)$	$P(F_3)$	$P(F_4)$	Sources
GSS	8.2×10^{-2}	1.6×10^{-2}	6.7×10^{-2}	1.42×10^{-10}	6.26×10^{-6}	This study
Direct MCS	8.6×10^{-2}	1.8×10^{-2}	6.8×10^{-2}	6.25×10^{-7}	6.25×10^{-6}	Low (1997)
Bound method based on FORM	7.0×10^{-2} $\sim 9.2 \times 10^{-2}$	2.4×10^{-2}	7.0×10^{-2}	1.05×10^{-9}	6.91×10^{-6}	Low (1997)

Table 8. Correlation coefficients among limit state functions of the four scenario failure events

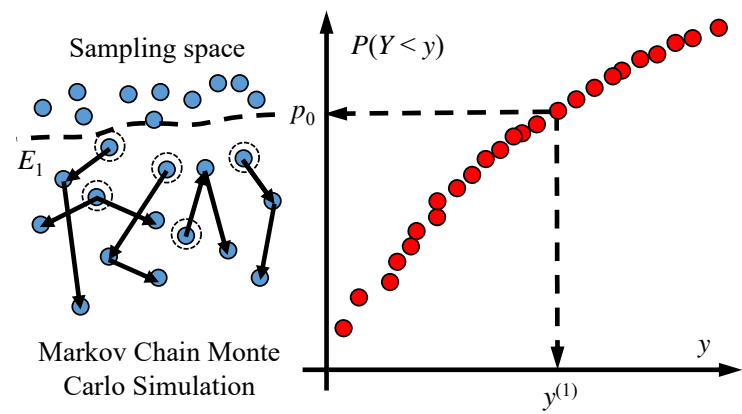| Failure events	F_1	F_2	F_3	F_4
F_1	1	0.404	0.379	0.452
F_2		1	0.296	0.798
F_3		Sym.	1	0.784
F_4				1

List of Figures:

Figure 1. Fault tree for system failure of slope stability
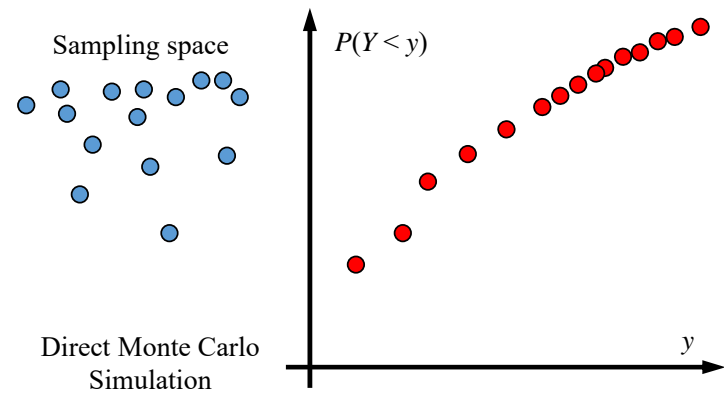
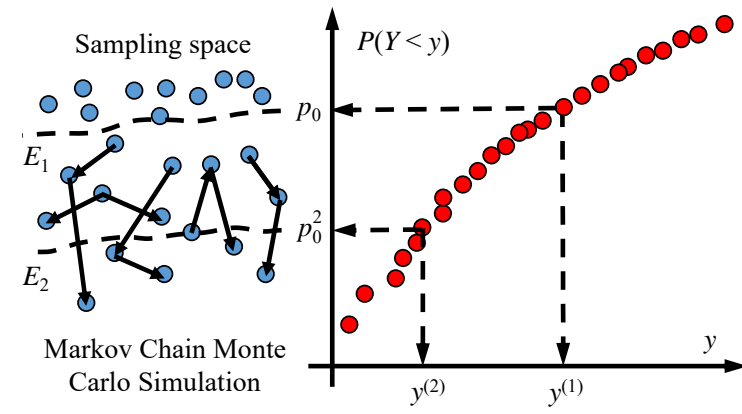(a) Level 0: direct Monte Carlo Simulation
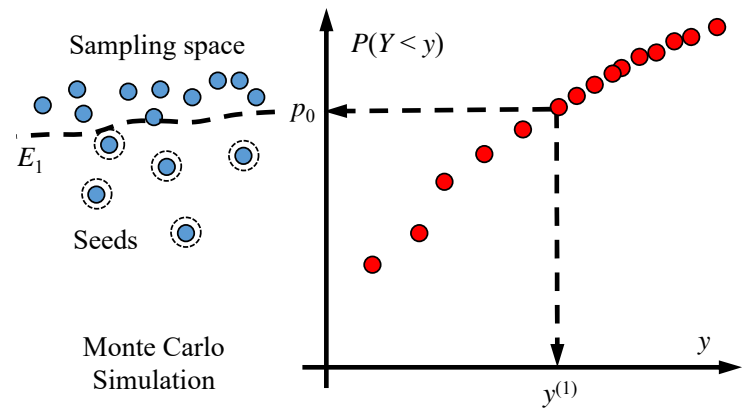
(b) Level 0: adaptive selection of $y^{(1)}$

(c) Level 1: Markov Chain Monte Carlo Simulation

(d) Level 1: adaptive selection of $y^{(2)}$

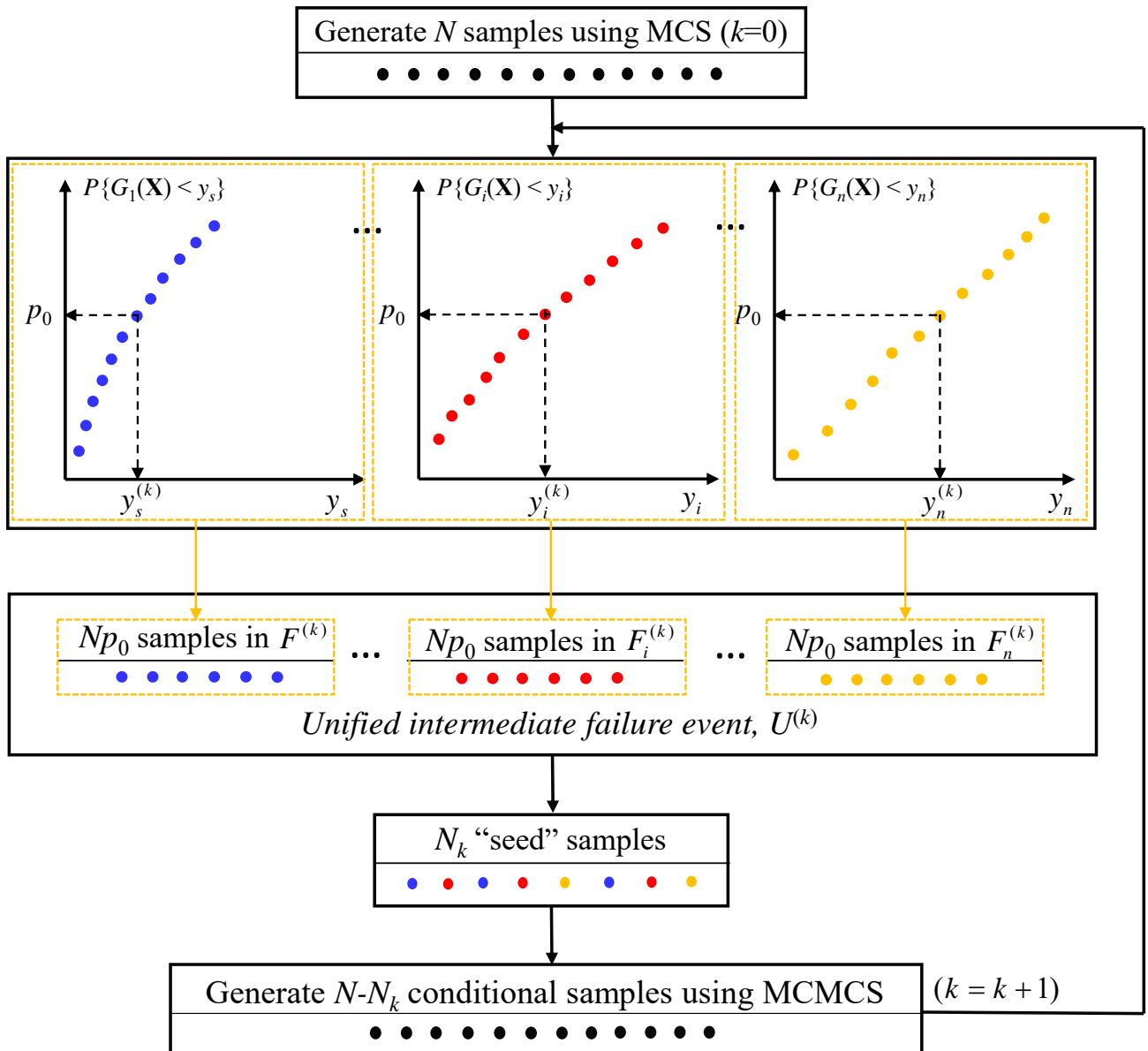**Figure 2.** Schematic diagram of Subset Simulation procedure (After Au et al. (2010) and Li et al. (2016c))

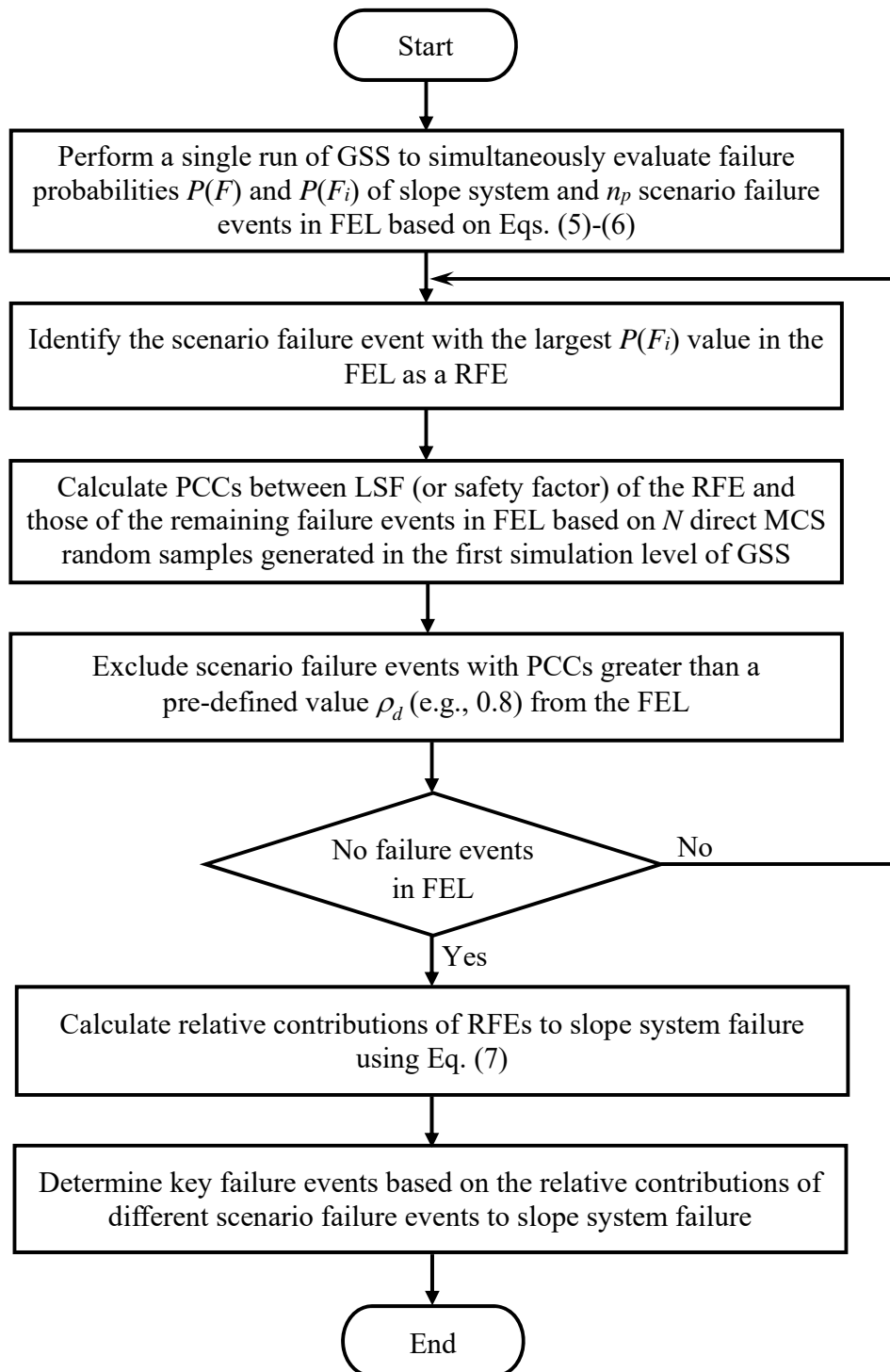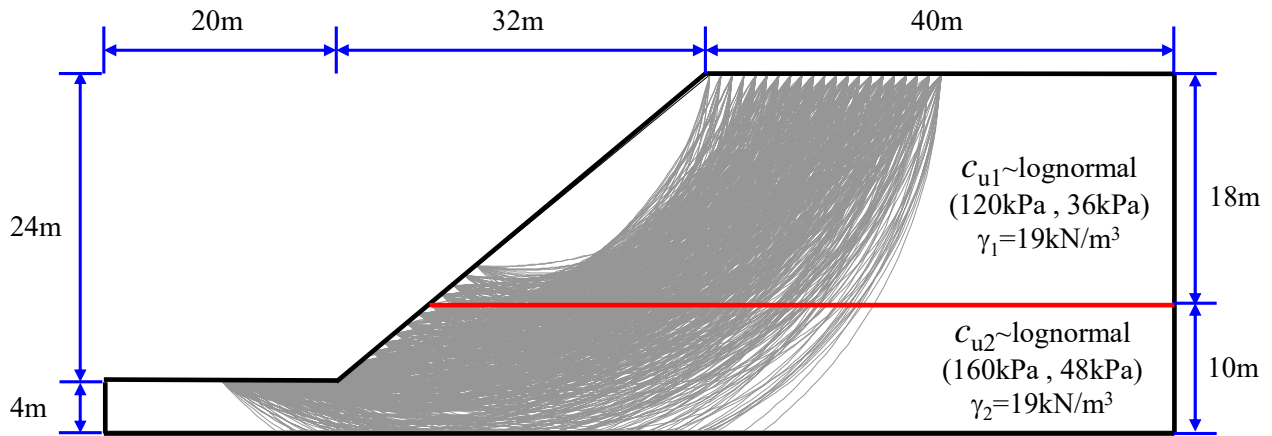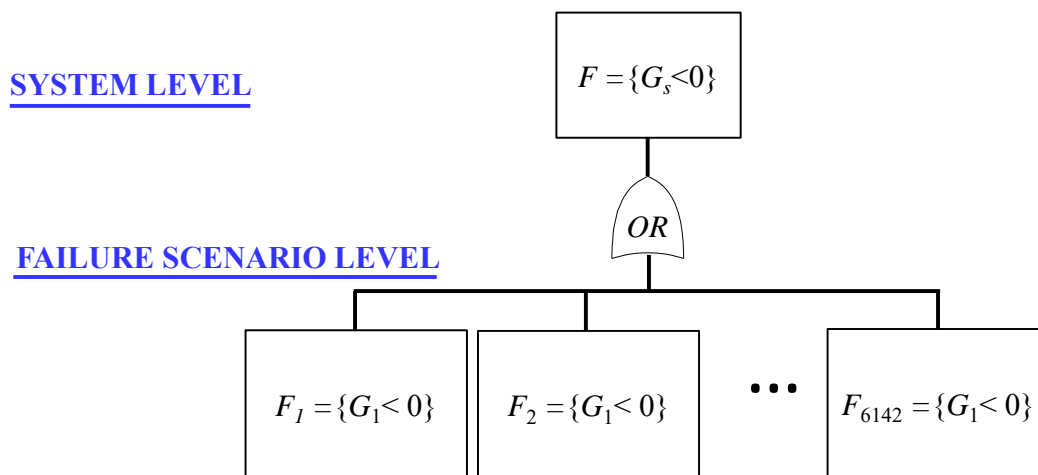**Figure 3.** Schematic diagram of Generalized Subset Simulation procedure

Figure 4. Implementation procedure of probabilistic network evaluation technique

(a) 6142 potential slip surfaces

$$F = \{G_s < 0\}$$

$$OR$$

FAILURE SCENARIO LEVEL

$$F_1 = \{G_1 < 0\} \quad F_2 = \{G_1 < 0\} \quad \bullet \bullet \bullet \quad F_{6142} = \{G_1 < 0\}$$

(b) Fault tree for system failure of the soil slope

Figure 5. Illustration of the soil slope example
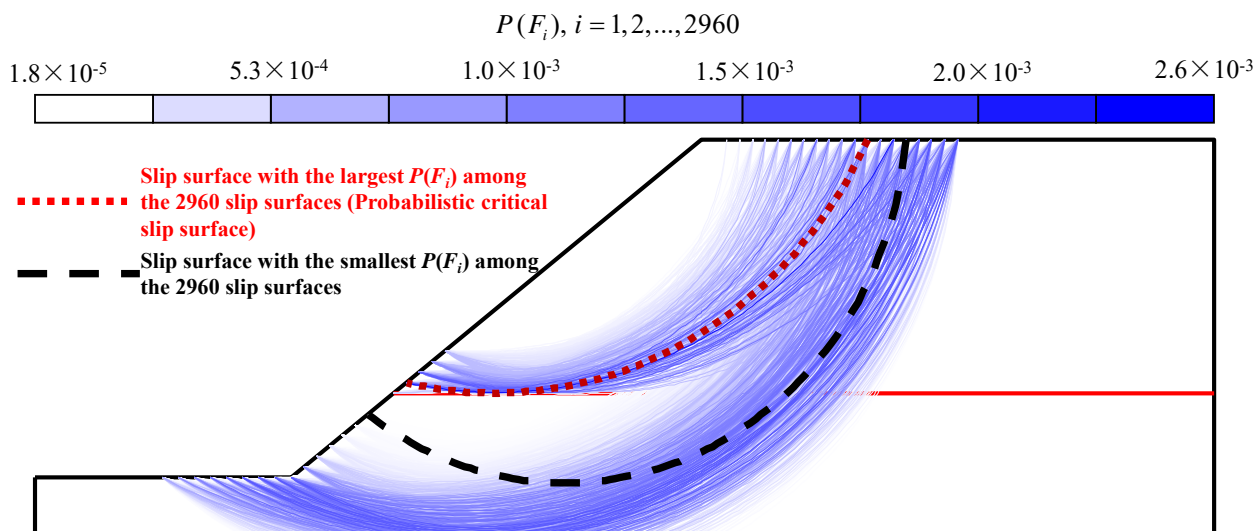
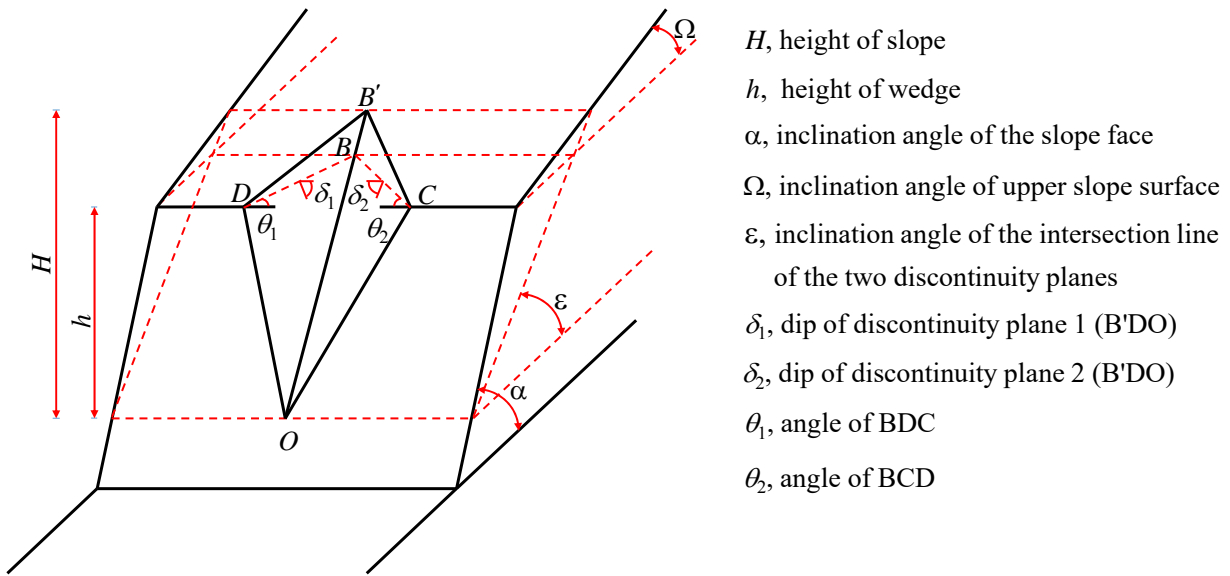**Figure 6.** Failure probabilities of 2960 scenario failure events

Figure 7. Two representative failure events identified by PNET method based on GSS results

Figure 8. Illustration of the rock slope example (After Low (1997) and Li et al. (2009))

H, height of slope

h, height of wedge

α, inclination angle of the slope face

Ω, inclination angle of upper slope surface

ε, inclination angle of the intersection line
    of the two discontinuity planes

δ_1, dip of discontinuity plane 1 (B'DO)

δ_2, dip of discontinuity plane 2 (B'DO)

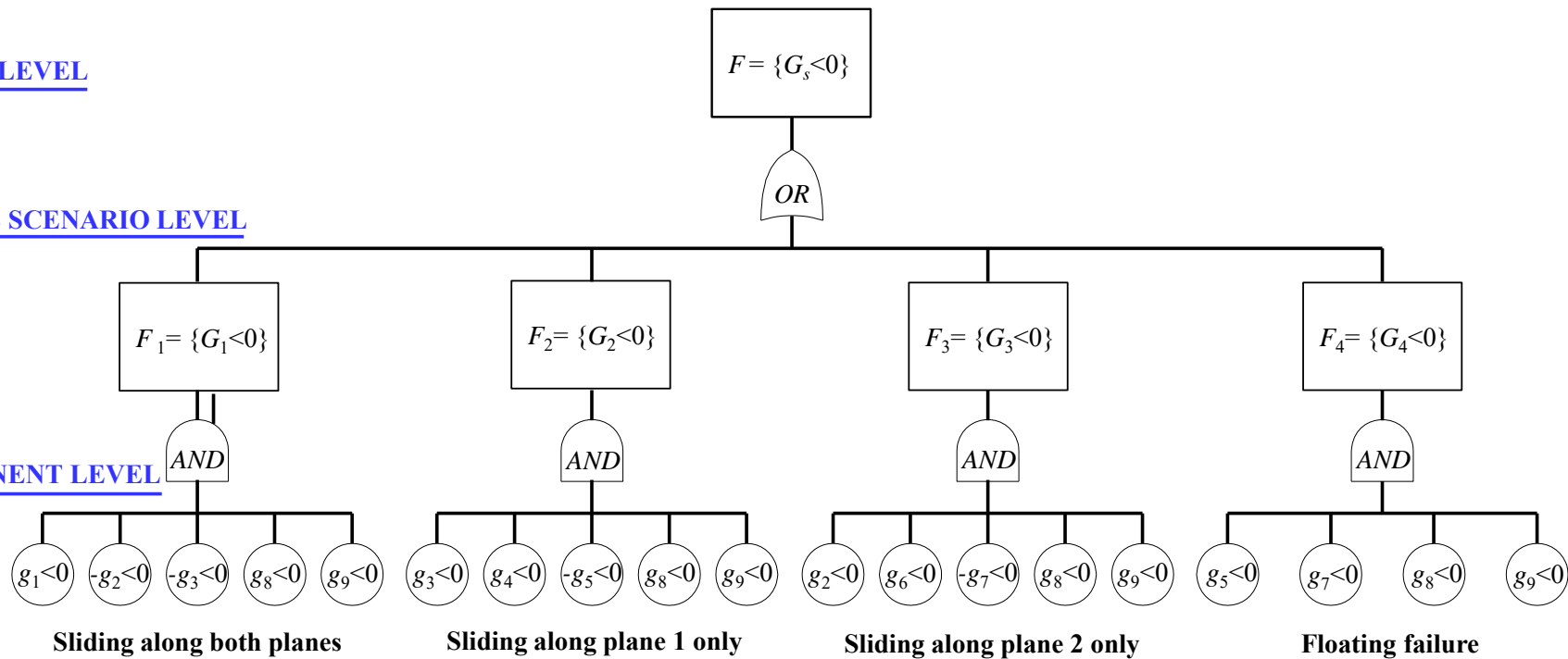θ_1, angle of BDC

θ_2, angle of BCD

Figure 9. Fault tree for system failure of the rock slope example (After Li et al. (2009))